A Tin(IV)−Ruthenium(II)−Tin(IV) Cyclic Porphyrin Trimer with Replaceable Chiral Linings

Simon J. Webb*,† and Jeremy K. M. Sanders‡

Department of Chemistry, The University of Sheffield, Sheffield S3 7HF, U.K., and University Chemical Laboratory, University of Cambridge, Lensfield Road, Cambridge CB2 1EW, U.K.

Received April 12, 2000

A series of cyclic metalloporphyrin trimers, **Ru(CO)(py)[Sn(carboxylate)$_2$]$_2$2**, having cavities lined with different carboxylate groups are synthesized by adding the appropriate carboxylic acids to the mixed trimer **Ru(CO)(py)[Sn(OH)$_2$]$_2$2**. This methodology provides ready access to a wide range of cavities lined with substituents possessing chirality or hydrogen-bonding groups. The potential of such systems is illustrated by synergistic binding of a hydroxypyridine to the Ru(II)−CO center and to the hydroxyl groups of a D-quinate-lined cavity. The effect of changing the carboxylate lining of the cavity on the course of epoxidation reactions catalyzed by these trimers is also reported.

As part of a project[1,2] aimed at achieving recognition and catalysis within the cavities of designed macrocycles, we describe here a series of cyclic metalloporphyrin trimers, **Ru(CO)(py)[Sn(carboxylate)$_2$]$_2$2**, that incorporate a ruthenium(II) carbonyl porphyrin and two tin(IV) porphyrins (see Chart 1). The tin centers are good attachment points for carboxylates, providing ready access to a wide range of cavities lined with substituents possessing chirality or other desired properties. We illustrate the potential of such systems by demonstrating synergistic binding of a hydroxypyridine to the ruthenium center and to the hydroxyl groups of a quinate attached to tin. The ruthenium center is also a potential catalytic site, and the effect of changing the carboxylate lining of the cavity in the course of epoxidation reactions catalyzed by these trimers is reported.

Tin(IV) metalloporphyrins have been known since the end of the last century and were among the first artificial metalloporphyrins synthesized.[3,4] Despite this early start, relatively little has been published since, perhaps because the coordination chemistry seemed well established. Tin(IV) porphyrins can be synthesized in high yield by heating a mixture of the free-base porphyrin and $SnCl_2 \cdot 2H_2O$ in pyridine at reflux in the presence of air. The postulated intermediate is an unstable tin(II) metalloporphyrin, which is rapidly air-oxidized to give the stable purple dichlorotin(IV) metalloporphyrin.[5]

Tin(IV) metalloporphyrins preferentially coordinate two anionic ligands, thus giving the metalloporphyrin no overall charge. Coordination of neutral ligands is rare and only occurs if the counterion associated with the metalloporphyrin is very weakly coordinating (for example, $CF_3SO_3^-$, NO_3^-, and ClO_4^-).[6,7] Tin(IV) metalloporphyrins are strongly oxophilic, as expected for such a highly charged metal ion. The dichloro complex, $SnCl_2$(Por), which is the compound isolated immediately after metalation, can be easily hydrolyzed (for example, during column chromatography) to give the dihydroxo complex, Sn(OH)$_2$(Por). The dihydroxo complex can then react with a variety of hydroxylic compounds, such as alcohols and carboxylic acids, to produce the corresponding alkoxide and carboxylate complexes. Simply stirring the dihydroxo complex and the appropriate acid together is sufficient to form the

Chart 1

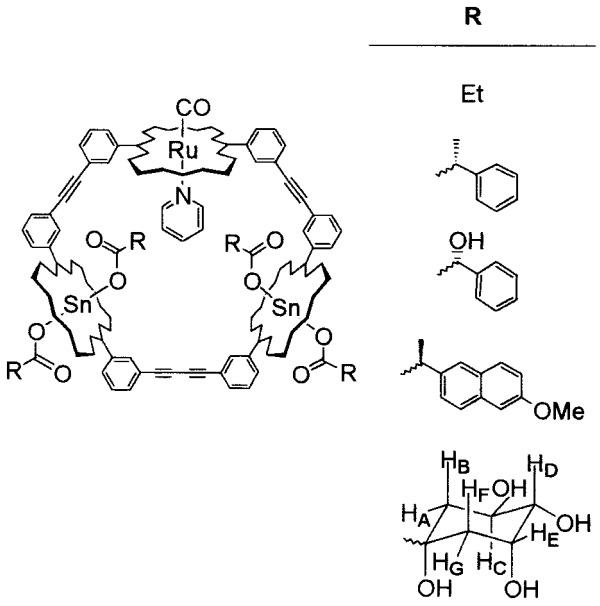

* Corresponding author. E-mail: S.J.Webb@sheffield.ac.uk.
† The University of Sheffield.
‡ University of Cambridge.

(1) (a) Sanders, J. K. M. In *Comprehensive Supramolecular Chemistry*; Atwood, J. L., Davies, J. E. D., Macnicol, D. D., Vögtle, F., Eds.; Elsevier: New York, 1996; Vol. 9, pp 131−164. (b) Anderson, H. L.; Sanders, J. K. M. *J. Chem. Soc., Perkin Trans. 1* **1995**, 2223 (c) Clyde-Watson, Z.; Bampos, N.; Sanders, J. K. M. *New J. Chem.* **1998**, *22*, 1135.
(2) Webb, S. J.; Sanders, J. K. M. *Inorg. Chem.* **2000**, *39*, 5912.
(3) Milroy, J. A. *J. Physiol.* (*London*) **1909**, *38*, 384.
(4) Tin(II) porphyrins were spectroscopically characterized many years ago (Whitten, D. G.; Yau, J. C.; Caroll, F. A. *J. Am. Chem. Soc.* **1971**, *93*, 2291) but were isolated only recently because of their high moisture and oxygen sensitivity: Barbe, J.-M.; Ratti, C.; Richard, P.; Lecomte, C.; Gerardin, R.; Guilard, R. *Inorg. Chem.* **1990**, *29*, 4126. They provide access to S=Sn(Por) and Se=Sn(Por): Guilard, R.; Ratti, C.; Barbe, J.-M.; Dubois, D.; Kadish, K. M. *Inorg. Chem.* **1991**, *30*, 1537.
(5) *The Porphyrins*; Dolphin, D., Ed.; Academic Press: New York; 1979; Vol. 1.
(6) Arnold, D. P.; Tiekink, E. R. T. *Polyhedron* **1995**, *14*, 1785.
(7) Smith, G.; Arnold, D. P.; Kennard, C. H. L.; Mak, T. C. W. *Polyhedron* **1991**, *10*, 509.

10.1021/ic0004129 CCC: $19.00
Published on Web 11/29/2000

carboxylate complex. The tin(IV) ion sits centrally within a slightly expanded porphyrin ring and coordination of the carboxylate anions is monodentate, in contrast to the bidentate binding mode found for group 4 metalloporphyrins.[5] These compounds are formed via Sn(Por)(OH)···HOOCR hydrogen-bonded intermediates, which can be detected by NMR spectroscopy.[8] Once formed, the carboxylate complexes are kinetically quite inert and, in the absence of acid, only exchange ligands over a period of weeks at room temperature.[9] Even upon the addition of an excess of CD_3CO_2H to $Sn(TPP)(O_2CCH_3)_2$, no exchange is observed after 5 h at room temperature.[10] The stability of these carboxylate complexes allows tin(IV) metalloporphyrins to be used as sensors for organic acids. Incorporation of tin(IV) metalloporphyrins into polymer membranes gave potentiometric probes that showed high sensitivity for salicylate and 2-hydroxybenzohydroxamate.[11,12] The stabilities of these complexes may generally be correlated with the pK_a values of the conjugate acids. As the acidities of the conjugate acids decrease, the anions become more electron rich, and thus better ligands, but also become prone to hydrolysis (for example, ethoxide).[13,14] Stronger acids yield complexes that are more stable to hydrolysis, but the anions coordinate to the tin much more weakly (for example, nitrate).[6,7] The carboxylate complexes seem to occupy the middle ground, and those with internal hydrogen bonds (such as salicylate and 2-hydroxybenzohydroxamate) seem to have unusually high stabilities, as does 9-anthroic acid.[8]

We have already demonstrated that the ruthenium centers in our porphyrin trimers can be used as recognition sites for pyridine-containing ligands.[2] However, the ruthenium porphyrin is also a potential catalytic site. Cyclopropanoation,[15] epoxide isomerization,[16] and oxidation[17,18] have all been catalyzed by ruthenium porphyrins. Ruthenium porphyrins have proved to be versatile catalysts for the oxidation of organic substrates. The synthesis of the bis(oxo)ruthenium(VI) porphyrin complex $Ru(TMP)(O)_2$ led to the discovery of catalytic epoxidation of alkenes by this complex in the presence of molecular oxygen.[17] More recently, iodosylbenzene[19] and heteroaromatic *N*-oxides[18] have been employed as more reactive oxygen sources than molecular oxygen. Heteroaromatic *N*-oxides have lower reactivity than reagents such as iodosylbenzene but do not degrade the catalyst or react with the substrate in the absence of catalyst. The most effective heteroaromatic *N*-oxide was 2,6-dichloropyridine *N*-oxide owing to the low basicity of 2,6-dichloropyridine and the inability of the free parent pyridine to coordinate to the ruthenium center and block further reaction.[18] With the use of 2,6-dichloropyridine *N*-oxide as the oxidant and $Ru(TMP)(O)_2$ as the epoxidation catalyst, yields of over 95% have been obtained for the epoxidation of various alkenes in benzene. We needed a system that was highly active yet selective enough to be compatible with the complex superstructure of our hosts. The 2,6-dichloropyridine *N*-oxide/$Ru(TMP)(O)_2$ system seemed to fulfill these criteria. In addition, since the *N*-oxide is present in a large excess relative to the catalyst, inactivation of the catalyst through dimerization to the inactive μ-oxo species is suppressed until the end of the reaction.[20]

The ease of synthesis and the relatively high kinetic and thermodynamic stabilities of the bound carboxylate ligands[8−10] implied that tin porphyrins might be useful units to effect changes in both the nature and the binding characteristics of the cavity of the **Ru(CO)M$_2$2** trimers.[2] Though the slow-exchange kinetics did not make the carboxylate−tin interaction a useful motif for binding substrates within the cavity, it opened the possibility, through variation of the nature of the bound carboxylate, of controlling the size and functionality of the cavity. Therefore, supramolecular interactions such as hydrogen bonding, van der Waals interactions, and electrostatic attraction might be used in the place of ligand−metal binding.

Results and Discussion

Synthesis. The presence of the ruthenium porphyrin subunit in **Ru(CO)[H$_2$]$_2$2** required that additional experimental precautions be taken during metalation with tin(II) chloride. The carbonyl ligand can be displaced by pyridine in the presence of light or heat, so there was some doubt as to whether the ruthenium carbonyl porphyrin would be stable under the tin insertion conditions. Initial attempts to insert tin by heating **Ru(CO)[H$_2$]$_2$2** with powdered $SnCl_2 \cdot 2H_2O$ in pyridine at reflux in air for 2 h often gave only impure products. However, shielding the reaction mixture from light during the tin insertion allowed **Ru(CO)(py)[SnCl$_2$]$_2$2** to be obtained without unwanted substitution at ruthenium. At this point, the product was the dichloro complex, which was converted to the dihydroxo complex during workup. The ^{1}H NMR spectrum of the crude **Ru(CO)(py)[SnCl$_2$]$_2$2** trimer showed Sn(por) meso-H at 10.70 ppm and Ru(por) meso-H at 9.48 ppm, though the meso-H region of the tin porphyrins showed some additional impurities, possibly resulting from partial hydrolysis. The complex had pyridine coordinated to the ruthenium center, the pyridyl α-protons giving a characteristic doublet at 0.68 ppm. After removal of the solvent under high vacuum, the residue was redissolved in chloroform and the solution was filtered through Celite to remove excess tin chloride. The chloroform solution was stirred with two portions of activity V alumina over 2 days, in a manner similar to that described by Arnold.[21] This afforded **Ru(CO)(py)[Sn(OH)$_2$]$_2$2** (Scheme 1), though often contaminated with excess pyridine, which had to be removed by recrystallization from dichloromethane/hexanes. The hydroxyl protons could be seen as broad features at −8.12 ppm (inside) and −7.83 ppm (outside) in the ^{1}H NMR spectrum. On average, one of the coordination sites was occupied with ethoxide, derived from the stabilizer in the chloroform solvent (−3.10 (t), −2.82 (q) ppm for CH_3CH_2O− inside the cavity; −2.67 (t), −2.43 (q) ppm for CH_3CH_2O− outside the cavity). The α-protons of the coordinated pyridine gave rise to a doublet at 0.84 ppm.

(8) Hawley, J. C.; Bampos, N.; Abraham, R. J.; Sanders, J. K. M. *Chem. Commun.* **1998**, 661.
(9) Arnold, D. P. *Polyhedron* **1988**, *7*, 2225.
(10) Sanders, J. K. M.; Hawley, J. C. Unpublished results.
(11) Kibbey, C. E.; Park, S. B.; Deadwyler, G.; Meyerhoff, M. E. *J. Electroanal. Chem. Interfacial Electrochem.* **1992**, *335*, 135.
(12) Badr, H. A.; Meyerhoff, M. E.; Hassan, S. S. M. *Anal. Chim. Acta* **1996**, *321*, 11.
(13) Tsai, C. C.; Chen, Y. J.; Chen, J. H.; Hwang, L. P. *Polyhedron* **1992**, *11*, 1647.
(14) Lin, H. J.; Chen, J. H.; Hwang, L. P. *Aust. J. Chem.* **1991**, *44*, 747.
(15) (a) Galardon, E.; Le Maux, P.; Simonneaux, G. *J. Chem. Soc., Chem Commun.* **1997**, 927. (b) Lo, W. C.; Che, C. M.; Cheng, K. F.; Mak, T. C. W. *J. Chem. Soc., Chem. Commun.* **1997**, 1205.
(16) Groves, J. T.; Ahn, K. H.; Quinn, R. *J. Am. Chem. Soc.* **1988**, *110*, 4217.
(17) (a) Groves, J. T.; Quinn, R. *Inorg. Chem.* **1984**, *23*, 3844. (b) Groves, J. T.; Quinn, R. *J. Am. Chem. Soc.* **1985**, *107*, 5790.
(18) Ohtake, H.; Higuchi, T.; Hirobe, M. *Heterocycles* **1995**, *40*, 867.
(19) Leung, T.; James, B. R.; Dolphin, D. *Inorg. Chim. Acta* **1983**, *79*, 180.
(20) Dimerization of sterically unhindered Ru^{IV}(Por)(O) to give inactive (μ-O)[Ru^{IV}(OH)(Por)]$_2$ can be prevented by adding a large excess of a coordinating ligand: Leung, W. H.; Che, C. M. *J. Am. Chem. Soc.* **1989**, *111*, 8812.
(21) Arnold, D. P. *Polyhedron* **1986**, *5*, 1957.

Scheme 1

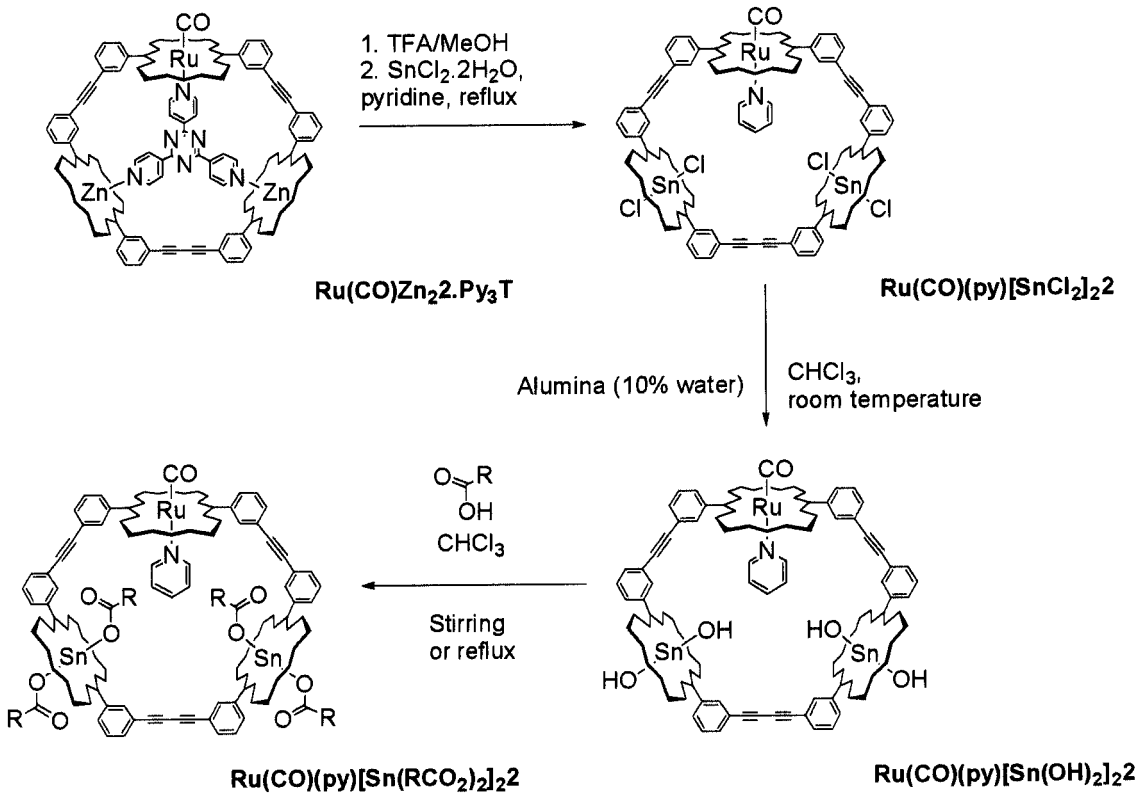

Attempts to synthesize the carboxylate complexes directly from the reactions of **Ru(CO)(py)[SnCl$_2$]$_2$2** with silver carboxylates led to partial replacement of the chloride anions but also resulted in side reactions at the ruthenium porphyrin units.

Binding Experiments. (a) Coordination of Carboxylates to Ru(CO)(py)[Sn(OH)$_2$]$_2$2. Stirring or heating **Ru(CO)(py)[Sn(OH)$_2$]$_2$2** with soluble carboxylic acids generally afforded the corresponding tetracarboxylate complexes quantitatively. This allowed access to a large range of trimers with different cavity linings. However, there were limits to the types of carboxylic acids that could be used. Diacids are known to bridge the exterior coordination sites to give polymers.[22] Polyhydric acids are not usually soluble in chloroform, but this problem could be circumvented by adding small amounts of methanol to the reaction mixture. Although methanol is a competing ligand, the corresponding methoxide complexes are not stable to substitution by carboxylic acids. The size of the acid is also important, as there must be enough space within the cavity for both of the interior carboxylates; attempts to coordinate the large podocarpate ligand (Chart 2) to the tin porphyrins of **Ru(CO)(py)[Sn(OH)$_2$]$_2$2** were unsuccessful.

Once synthesized, the **Ru(CO)(py)[Sn(carboxylate)$_2$]$_2$2** trimers were sensitive to large amounts of hydroxylic solvents, such as methanol, because these displaced the carboxylate ligands. Standard column chromatography could not be used to purify the complexes, since the tin centers coordinated irreversibly to silica gel and alumina displaced the bound carboxylates to regenerate **Ru(CO)(py)[Sn(OH)$_2$]$_2$2**. However the complexes could be recrystallized from dichloromethane/hexanes, and washing with dry diethyl ether removed excess acid.

A **Ru(CO)(py)[Sn(carboxylate)$_2$]$_2$2** complex has three different coordination environments: (i) the interior coordination site of the ruthenium porphyrin, only the interior site being available for incoming ligands, since the exterior position is blocked by CO; (ii) the exterior coordination sites of the tin porphyrins; (iii) the interior coordination sites of the tin porphyrins, interior ligands displaying distinctly upfield chemical shifts in the ^{1}H NMR spectrum relative to exterior ligands, as they are shielded by the ring currents of all three porphyrins of the host.

Chart 2

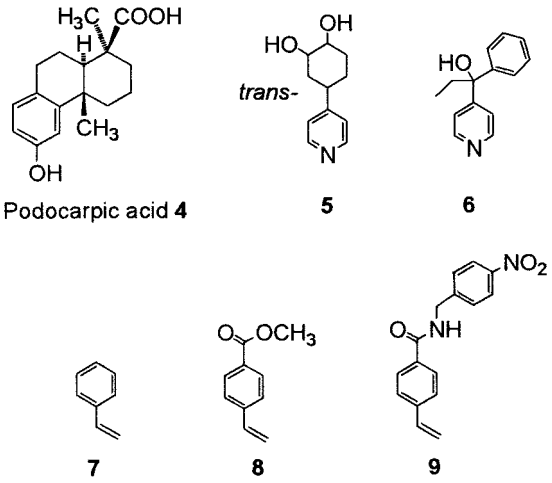

The carboxylic acids we bound to **Ru(CO)(py)[Sn(OH)$_2$]$_2$2** were selected to impart specific characteristics to the cavity of the trimer. The versatility of this method and characteristics of the complexes were investigated initially with simple acids (Chart 1).

Stirring a mixture of **Ru(CO)(py)[Sn(OH)$_2$]$_2$2** and propionic acid together for 15 min was found to be sufficient to exchange the hydroxyls for propanoates. Removal of the chloroform solvent and drying under high vacuum afforded the **Ru(CO)-**

(22) Buchler, J. W. In *Porphyrins and Metalloporphyrins*; Smith, K. M., Ed.; Elsevier: New York, 1975; Chapter 5, p 171.

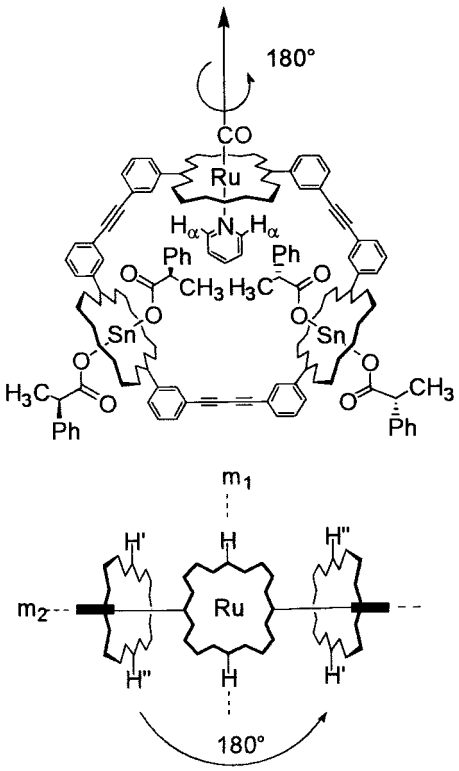

Figure 1. Illustration of the symmetry of the chiral **Ru(CO)(py)[Sn(carboxylate)$_2$]$_2$2** trimers.

(py)[Sn(propanoate)$_2$]$_2$2 trimer. The proton NMR spectrum of this compound showed a single tin porphyrin meso-H resonance at 10.57 ppm and a single ruthenium porphyrin meso-H resonance at 9.49 ppm. In the upfield region, a series of triplets and quartets denoted the bound propanoates (−1.58 (t), −1.11 (q) ppm for exterior propanoate; −2.14 (t), −1.72 (q) ppm for interior propanoate. Integration of the resonances of the coordinated propanoates showed that the interior positions were occasionally incompletely occupied. This was due to the incomplete hydrolysis of these positions during the synthesis of **Ru(CO)(py)[Sn(OH)$_2$]$_2$2**. By using propanoate as a probe, we were able to fine-tune the hydrolysis period and achieve complete conversion. The presence of an unexpected 5 Hz doublet at 0.7 ppm and triplet at 4.1 ppm showed that pyridine was still coordinated to the ruthenium center, despite the presence of excess acid. This was also found for all of the other **Ru(CO)(py)[Sn(carboxylate)$_2$]$_2$2** trimers.

Coordination of a chiral ligand to a tin porphyrin should yield a trimer with a chiral cavity. 2-Phenylpropanoate was selected because both enantiomers are commercially available and there are large size differences among the substituents (Ph > Me > H) at the chiral carbon. It is also small enough that both interior ligands can be accommodated within the cavity but large enough to project over the potential active site at the ruthenium center. A mixture of **Ru(CO)(py)[Sn(OH)$_2$]$_2$2** and 4.1 equiv of (*R*)-(−)-2-phenylpropanoic acid was heated in chloroform briefly before the solvent was removed under reduced pressure. To remove excess acid, the solid was washed with dry diethyl ether after recrystallization from dichloromethane/hexanes.

The proton NMR spectrum of this trimer was much more complicated than that observed for the propanoate complex. The chiral ligands effectively remove a plane of symmetry from the complex and instead introduce a C_2 axis of rotation (Figure 1). Thus all the protons except those on the two planes shown in Figure 1 gave rise to pairs of resonances. Therefore, there were two tin meso-H resonances (10.43, 10.45 ppm) but only one ruthenium meso-H resonance (9.47 ppm). The only clear resonance of the pyridine ligand was a doublet at 0.63 ppm, due to the pyridyl α-protons. The resonances of the interior and exterior (*R*)-2-phenylpropanoate ligands were clearly resolved. The resonances for the phenyl rings appeared in a relatively clear part of the spectrum, 4.0−6.5 ppm, and the α-protons were found as quartets at 0.38 ppm (exterior) and −0.31 ppm (interior). The exterior and interior resonances of the α-methyls appeared as doublets at −1.15 and −1.83 ppm, respectively. The relatively simple appearance of the (*R*)-2-phenylpropanoate resonances of the ligand suggested rapid rotation about both the CH−Ph and Sn−O bonds.

Mandelate, while retaining the spectroscopically useful phenyl group of 2-phenylpropanoate, now has an α-hydroxyl group (Chart 1). This was to act as a recognition unit for ligands bound to the ruthenium center. The α-hydroxyl group might also internally hydrogen-bond to the carbonyl oxygen of the carboxylate group and thus eliminate one degree of free rotation in the ligand. **Ru(CO)(py)[Sn((*R*)-mandelate)$_2$]$_2$2** was synthesized by the same method as that used for the chiral **Ru(CO)(py)[Sn((*R*)-2-phenylpropanoate)$_2$]$_2$2** trimer. After recrystallization, the proton NMR spectrum showed a large chemical shift difference between the different tin meso-H resonances (0.69 ppm). This may be the result of the internal α-OH···O=C hydrogen bond restricting intraligand rotation. Otherwise, the overall appearance of the spectrum was similar to that observed for the 2-phenylpropanoate complex, the exterior and interior α-protons of the carboxylate appearing as singlets at 1.65 and 1.27 ppm, respectively.

Naproxenate ((*S*)-(+)-6-methoxy-α-methyl-2-naphthaleneacetate) is larger than either mandelate or 2-phenylpropanoate but still small enough to fit within the cavity. Although this ligand lacks any hydroxylic functions, the methoxy group on the 6-position of the naphthyl ring could act as a hydrogen-bond acceptor (Chart 1). **Ru(CO)(py)[Sn((*S*)-(+)-6-methoxy-α-methyl-2-naphthaleneacetate)$_2$]$_2$2** was synthesized using the method employed for **Ru(CO)(py)[Sn((*R*)-mandelate)$_2$]$_2$2**. The proton NMR spectrum showed coordination of the carboxylates (the exterior and interior α-methyls gave rise to doublets at 1.03 and 1.73 ppm, respectively) and two clearly separated tin porphyrin meso-H resonances (10.27, 10.33 ppm). The naphthyl ring proton resonances overlapped and gave a complex pattern between 4.0 and 7.1 ppm.

It was unclear whether enough functionality was present within the preceding chiral trimers to bind substrates effectively and whether this functionality was projecting sufficiently deeply into the cavity. D-(−)-Quinate ((1*R*,3*R*,4*R*,5*R*)-(−)-quinate) appeared to offer a solution. Although this ligand no longer has an aromatic group to act as an ^{1}H NMR probe, it is rigidly defined by the cyclohexane ring and the α-hydroxyl group. Quinate has hydroxyl groups at the 3-, 4-, and 5-positions, providing many hydrogen-bonding sites in the center of the cavity. Molecular modeling also suggested that the 4-hydroxyl groups of the interior quinates may be able to hydrogen-bond to each other. The insolubility of D-quinic acid in chloroform required a slight modification of the experimental procedure. Heating a mixture of **Ru(CO)(py)[Sn(OH)$_2$]$_2$2** and D-quinic acid in chloroform/methanol (2:1), followed by removal of the solvent under reduced pressure, gave the quinate complex, which then proved to be soluble in chloroform. The proton NMR spectrum of this host was different from those obtained with the other chiral acids, for in this case there was no separation of the tin porphyrin meso-H chemical shifts. The eight $-CH_2-$

resonances of the quinate groups could be observed in the region −2.3 to −0.7 ppm, though the −C*H*OH− resonances were masked by the side chains on the porphyrin. Despite the complexity of the ^{1}H NMR spectrum, it was almost completely assigned through a COSY NMR experiment. This showed that the interior and exterior quinate ligands gave rise to two analogous coupling patterns, though the chemical shifts were quite different. However, proton H_E, with dihedral angles of 60° to its vicinal partners (Chart 1), gave only a weak cross-peak in the COSY spectrum. The E protons of the interior quinates could be found, but the cross-peaks to the E protons of the exterior quinates were too weak to be detected.

Instead of hydrogen bonding, other aspects of enzymatic binding and catalysis may be explored by using different types of carboxylates to line the cavity. Mercaptocarboxylates might be used for nucleophilic catalysis, $\pi-\pi$ interactions might be studied using aromatic carboxylates, and pyridinium carboxylates could be used to generate charged cavities. In a preliminary experiment aimed toward investigating the latter case, 1-(carboxymethyl)pyridinium chloride and **Ru(CO)(py)[Sn(OH)$_2$]$_2$2** were stirred together in a chloroform/methanol mixture. However, instead of the carboxylate coordinating to the host, the chloride counterion coordinated to the tin centers to regenerate **Ru(CO)(py)[SnCl$_2$]$_2$2** and produced the 2-(1-pyridinium)acetate zwitterion as a byproduct.

(b) Binding of Pyridines to Chiral Ru(CO)(py)[Sn(carboxylate)$_2$]$_2$2 Complexes. (i) Binding of 4-Methanolpyridine to Chiral Ru(CO)(py)[Sn(D-quinate)$_2$]$_2$2. The cavity of the chiral quinate trimer was designed to present a rich hydrogen-bonding environment for any ligand bound to ruthenium. Those ligands that can hydrogen-bond to the lining of the cavity should display higher constants for binding to the quinate trimer than those without hydrogen-bonding functionalities. Since the ruthenium porphyrin was already bound to pyridine, the best way to determine the magnitude of any host−ligand hydrogen bonding was through a competition experiment between pyridine (Py), which has no hydrogen-bonding ability, and the hydrogen-bonding pyridyl ligand (Py_{OH}). The presence of a large excess of pyridine ensured that all trimers had pyridine bound initially. Subsequent addition of aliquots of the competing ligand to the host/pyridine mixture allowed the ratio of host·Py to host·Py_{OH} to be determined at each individual Py:Py_{OH} ratio. The relative binding constant (K_{rel}) could then be obtained from the equation

$$K_{rel} = \frac{[\text{host}\cdot Py_{OH}][Py]}{[\text{host}\cdot Py][Py_{OH}]}$$

Proton NMR spectroscopy was the most convenient method for measuring this ratio, as pyridine ligands bound to ruthenium porphyrins are in slow exchange on the NMR time scale. The proton NMR spectrum of the quinate trimer was very complex and presented few windows in which such a small change in the overall spectrum could be measured. However, the pyridyl α-protons of the bound pyridine occupied a relatively clear region around 0.6 ppm. Therefore, the competing pyridyl ligand was chosen so that its pyridyl α-protons displayed chemical shifts distinct from those of the pyridyl α-protons of pyridine. If both ligands bind to the ruthenium center with equivalent porphyrin−pyridine distances, this chemical shift difference should be preserved in the complex and both sets of signals should be resolved in the proton NMR spectrum. Molecular modeling indicated that 4-methanolpyridine, 4-ethanolpyridine, and 3-propanolpyridine should all be able to participate in hydrogen bonding to the quinate groups, but only 4-methanolpyridine had chemical shifts of the α-protons (8.35 ppm) sufficiently different from those of pyridine (8.60 ppm) that resolution in the proton NMR spectrum was a realistic expectation.[23]

Initially, the intrinsic difference in the binding affinities of these ligands for a ruthenium monomer in $CDCl_3$ had to be determined. This also allowed the feasibility of monitoring binding by ^{1}H NMR spectroscopy to be established. Our standard ruthenium monomer **Ru(CO)3** was not suitable, since the pyridine adduct had three different atropisomers, each with slightly different chemical shifts.[2,24] This led to overlapping signals for the bound pyridine and did not allow any resolution between the two different pyridyl complexes. The problem was avoided by switching to symmetrical carbonyl(tetrakis(3,5-di-*tert*-butylphenyl)porphinato)ruthenium(II).

By analogy with the values known for zinc porphyrins,[25] the ratio between the constants for binding of 4-methanolpyridine and pyridine to a ruthenium(II) porphyrin was anticipated to be approximately 1.5:1, with the more basic 4-methanolpyridine binding more tightly. A 10-fold (based upon porphyrin) excess of pyridine was added to a solution of the ruthenium porphyrin (4.20 μmol in 0.500 mL of $CDCl_3$), and aliquots of a solution of 4-methanolpyridine (20 equiv total in 200 μL of $CDCl_3$) were added. A 250 MHz ^{1}H NMR spectrum of the mixture was recorded after each addition. The Ru(Por)·Py:Ru(Por)·$PyCH_2$-OH ratio was most easily measured from the integration of the γ-proton (pyridine) and β-proton (pyridine + 4-methanolpyridine) resonances, though the spectra showed the two α-protons of the complexed pyridine ligands were resolved (doublets at 1.66 (Py) and 1.61 ppm ($PyCH_2OH$)) even at 250 MHz. The product of the Ru(Por)·$PyCH_2OH$:Ru(Por)·Py and Py:$PyCH_2$-OH ratios gave a relative binding constant of 2.2 ± 0.5, which was similar to that expected.[25]

The same method was used to determine the relative constants for binding of these two ligands to the quinate trimer (Scheme 2). A 20-fold excess of pyridine was used because if a higher binding constant were observed due to hydrogen bonding, then lower proportions of 4-methanolpyridine to pyridine would have to be used to ensure a measurable trimer·Py:trimer·$PyCH_2OH$ ratio. In addition, the proton NMR spectra were recorded at 500 MHz to improve the dispersion of the bound α-proton resonances. The pyridine:4-methanolpyridine ratio was determined directly by integration of the spectra.

The behavior of the quinate trimer upon addition of 4-methanolpyridine was quite different from that of the monomer. The α-proton resonances of the bound pyridyl ligands actually overlapped, making resolution impossible. However, there was a marked downfield shift of the ruthenium meso-H resonance, from 9.48 ppm (pyridine bound) to 9.57 ppm (4-methanolpyridine bound). This, in conjunction with the smaller upfield shifts shown by the α-protons of 4-methanolpyridine in the adduct, suggests that the 4-methanolpyridine is being pulled away from the porphyrin plane, perhaps due to the effects of hydrogen bonding. The trimer·Py:trimer·$PyCH_2OH$ ratio was easily determined by integration of the ruthenium meso-H signals. As with the monomer, the product of the trimer·$PyCH_2OH$:trimer·Py and Py:$PyCH_2OH$ ratios gave the relative binding constant.

(23) Pouchert, C. J.; Behnke, J. *The Aldrich Library of ^{13}C and ^{1}H FT NMR Spectra*, 1st ed.; Aldrich: Milwaukee, WI, 1993; Parts 1 and 2.
(24) Marvaud, V.; Vidal-Ferran, A.; Webb, S. J.; Sanders, J. K. M. *J. Chem. Soc., Dalton Trans.* **1997**, 985.
(25) (a) Levy, E. G. Ph.D. Thesis, University of Cambridge, 1996. (b) Izatt, R. M.; Bradshaw, J. S.; Pawlak, K.; Bruening, R. L.; Tarbet, B. J. *Chem. Rev.* **1992**, *92*, 1261.

Scheme 2

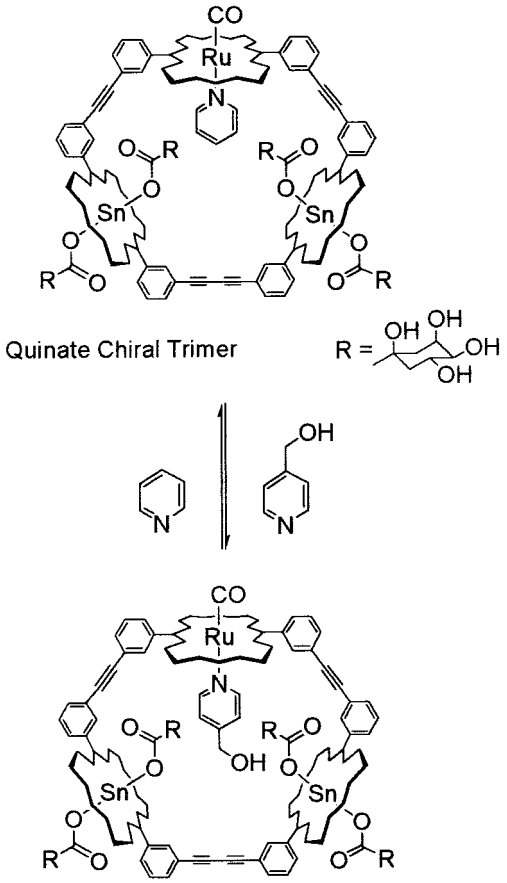

This showed that the quinate trimer displayed a 20-fold preference for binding 4-methanolpyridine instead of pyridine.

Therefore, a net enhancement of (9 ± 2)-fold for the binding of 4-methanolpyridine to the quinate trimer over the ruthenium monomer was observed. The chemical shifts of the interior quinate groups were considerably shifted upon binding 4-methanolpyridine, while the exterior quinate groups were left unchanged. This is consistent with hydrogen bonding to the interior quinate residues causing the stronger binding (Figure 2). The free energy calculated for the exchange of pyridine with 4-methanolpyridine is 5.4 ± 0.6 kJ/mol. This is lower than the value of 12−25 kJ/mol expected for hydrogen bonding between hydroxyl groups[26] and suggests that restriction of the rotation of the quinate ligands about the tin−carboxylate axis may enforce a high entropic cost on any hydrogen-bonding interactions. The 500 MHz NOESY spectrum of the trimer·$PyCH_2$-OH complex showed no cross-peaks between the resonances of the pyridyl ligands and the interior carboxylates.

(ii) Binding of Racemic Pyridines to Chiral Ru(CO)(py)-[Sn(carboxylate)$_2$]$_2$2 Complexes. The binding of chiral acids to **Ru(CO)(py)[Sn(OH)$_2$]$_2$2** imparted chirality to the cavity, and we wanted to test the stereoselectivity of some of these resultant chiral hosts by binding racemic pyridyl guests. Racemic (±)-4-(4-pyridyl)-*trans*-cyclohexane-1,2-diol (**5**) and (±)-1-phenyl-1-pyridylpropan-1-ol (**6**) (Chart 2) were added to solutions of the chiral trimers in $CDCl_3$, and the resulting mixtures were analyzed by NMR spectroscopy to determine the ratio of diastereomers. The results from these studies provided some insight into the factors important in discriminating between racemic guests or between transition states within a chiral cavity.

(26) March, J. *Advanced Organic Chemistry*, 4th ed.; Wiley-Interscience: New York, 1992; Chapter 3, p 76.

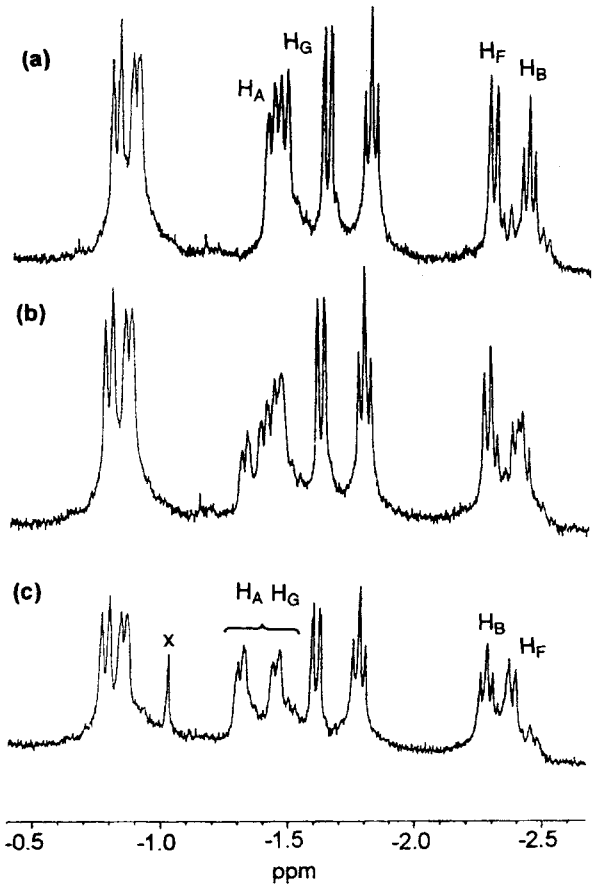

Figure 2. Changes observed in the upfield region of the ^{1}H NMR spectrum when 4-methanolpyridine is added to a mixture of **Ru(CO)-(py)[Sn(D-quinate)$_2$]$_2$2** and pyridine in $CDCl_3$. (a) No 4-methanolpyridine is added. Resonances due to the methylene protons of both the internal (labeled) and external quinate groups are visible in this part of the spectrum. (b) With a pyridine:4-methanolpyridine ratio of 20.2:1, the peaks of the new 4-methanolpyridine complex start to appear in the spectrum. (c) With a pyridine:4-methanolpyridine ratio of 1.33:1, the spectrum is now largely that of the 4-methanolpyridine-containing species. This spectrum shows that though the internal quinate groups experience a significant change, coordination of 4-methanolpyridine has little effect upon the chemical shift of the external quinate groups.

All combinations of racemic pyridine and host were found to give 1:1 diastereomeric mixtures, despite molecular modeling suggesting that for several of the host/guest pairs there should have been significant interaction between the carboxylate and pyridyl moieties. We believe rotation about the Sn−O axis to be the reason for this low selectivity. The relatively simple appearance of the NMR spectra suggested that this rotation is rapid at room temperature, preventing the cavities from having defined chiral shapes.

Despite their lack of selectivity, the complexes of **Ru(CO)-(py)[Sn(D-quinate)$_2$]$_2$2** with **5** and **6** showed some unexpected effects. The mixture of **5** with the quinate trimer gave a very complex proton NMR spectrum with few assignable resonances. Four ruthenium meso-H resonances were observed, while the ligand pyridyl α-protons gave an ill-resolved multiplet between 0.78 and 0.85 ppm. The rest of the spectrum could not be assigned, since the resonances of the cyclohexane-1,2-diol ring and the quinate groups overlapped in both the one- and two-dimensional spectra. Though the spectrum defied detailed interpretation, the smaller upfield shifts of the pyridyl α-protons compared to those for the analogous complex of **Ru(CO)(py)-[Sn((*R*)-mandelate)$_2$]$_2$2** with **5** (0.49 ppm) suggested that, in this case, as with 4-methanolpyridine, there may be hydrogen-

bonding interactions with the quinate groups of the cavity. The mixture of **6** with **Ru(CO)(py)[Sn(D-quinate)$_2$]$_2$2** also gave a complicated spectrum. The pyridyl α-protons of the ligand appeared as two unresolved multiplets at 0.60 and 0.64 ppm. This suggested some hydrogen bonding, since the pyridyl α-protons are found at 0.50 ppm in the spectrum of the analogous complex of **6** with **Ru(CO)(py)[Sn((*R*)-mandelate)$_2$]$_2$2**. However, the resonances of the phenyl groups were well resolved in a clear region of the spectrum and provided the key to the interpretation of this spectrum. The 500 MHz gradient NOESY and COSY spectra of this mixture revealed an unexpected coupling pattern. Rather than two diastereomeric complexes, four individual complexes could be identified. Two of these could be easily identified as the diastereomeric adducts of (±)-1-phenyl-1-pyridylpropan-1-ol with the quinate trimer, present in an approximately 1:1 ratio. The remaining two complexes in the mixture were found to have additional pyridyl α- and *β*-proton resonances at 1.23 and 5.04 ppm, respectively. By comparison to those of the pyridine complex of the ruthenium monomer **Ru(CO)3** (1.23 and 5.13 ppm, respectively), these can be assigned to (±)-1-phenyl-1-pyridylpropan-1-ol coordinated to the exterior of the cavity. Thus, the exterior CO must have been displaced by (±)-1-phenyl-1-pyridylpropan-1-ol. No other combination of host and racemic pyridyl ligand showed any trace of this displacement phenomenon. Repetition of this experiment with the exclusion of light gave the same mixture, with exactly the same ratio of products. A possible explanation is that hydrogen bonding of (±)-1-phenyl-1-pyridylpropan-1-ol to the quinate groups within the cavity pulls this ligand away from the porphyrin plane and causes it to pull the ruthenium ion, normally displaced toward the carbonyl,[27] into the plane of the porphyrin ring. This leads to weakening of the Ru−CO bond and therefore to susceptibility of the carbonyl to substitution. It remains to be seen if this could be used as a general approach to nonphotolytic replacement of the CO group.

Catalysis Experiments. In a series of preliminary experiments, both **Ru(CO)(py)[Sn((*R*)-2-phenylpropanoate)$_2$]$_2$2** and **Ru(CO)(py)[Sn((*R*)-mandelate)$_2$]$_2$2** were tested as catalysts for the enantioselective epoxidation of prochiral alkenes.

Although both carboxylate ligands are of similar size and shape, the (*R*)-mandelate groups have a hydroxyl as a possible binding site, and it was hoped that using substrates designed to interact with the hydroxyl moiety would lead to enantioselectivity. Modeling was used to select or design alkenes and carboxylates so the interaction between the substrate and the cavity would be maximized. Molecular modeling suggested that hydrogen-bond donors/acceptors at the para position of the styryl group may be able to interact with the hydroxyl groups of the chiral mandelate trimer. Furthermore, an inclined aromatic ring placed slightly further out from the styryl core may be able to *π*-stack with the phenyl ring of the mandelate ligands. Therefore, in addition to styrene **7**, two other substrates were tested (Chart 2). Methyl 4-vinylbenzoate (**8**) has an ester group as a hydrogen-bond acceptor, and *N*-(4-nitrobenzyl)-4-vinylbenzamide (**9**) has an amide group as a hydrogen-bond acceptor/donor with a *p*-nitrophenyl ring as a *π*-acceptor.

The method of Hirobe et al. was used for the epoxidation experiments, with a slight modification.[18] The **Ru(CO)(py)[Sn(carboxylate)$_2$]$_2$2** trimers have pyridine tightly coordinated to the ruthenium. To displace the pyridine and initiate the reaction, a small amount (4 equiv relative to the ruthenium porphyrin) of *m*-CPBA (86% purity) had to be added. The UV−visible spectrum showed that a Ru^{VI}(O)$_2$(por) species was formed in the process. Insufficient *m*-CPBA was present to significantly affect the result of the oxidation experiment, and carboxylate exchange at tin was sufficiently slow not to be a major problem.[8,10] In a further control experiment, a 1:20 mixture of Sn(TPP)(propanoate)$_2$ and 2,6-dichloropyridine *N*-oxide in $CDCl_3$ showed no displacement of the propanoate by the *N*-oxide.

Initially, to test the reaction conditions, styrene was epoxidized with **Ru(CO)3**. This reaction was found to proceed rapidly and was essentially complete after 3 h, producing styrene oxide in 87% yield (a turnover number of 157).

Epoxidations of styrene in the presence of **Ru(CO)(py)[Sn((*R*)-2-phenylpropanoate)$_2$]$_2$2** and **Ru(CO)(py)[Sn((*R*)-2-mandelate)$_2$]$_2$2** did not result in any observable enantiomeric excesses. At first inspection, this might not be entirely unexpected, since styrene has no binding functionality and reaction can occur just as easily on either the exterior or the interior face of the cavity. However, the complete lack of enantioselectivity did imply that either reaction is prevented from occurring inside the cavity or chiral induction within the cavity is so weak that the substrate has no preferred direction of attack on the catalytic center. The chemical yields, based on the amount of styrene consumed, were low, at 20% and 53%, respectively.

When methyl 4-vinylbenzoate was epoxidized with the chiral mandelate trimer, a moderate yield of the epoxide (46%) was obtained, but once again no enantiomeric excess was observed.

Epoxidation of *N*-(4-nitrobenzyl)-4-vinylbenzamide with **Ru(CO)(py)[Sn((*R*)-2-mandelate)$_2$]$_2$2** was hampered by the limited solubility of the substrate in benzene. However, since a significant amount of the substrate was soluble, it was hoped that the dissolved benzamide would be able to exchange with the remaining undissolved substrate. Both the soluble and the insoluble product fractions were analyzed. No enantiomeric excess was observed in either fraction, and the overall chemical yield was only 11%.

These results, in conjunction with the lack of selectivity observed toward racemic pyridines, suggest that the cavities of the current range of chiral **Ru(CO)(py)[Sn(carboxylate)$_2$]$_2$2** trimers are not sufficiently structured to provide any significant enantioselectivity, irrespective of the presence or absence of any binding interactions within the cavity. A rigid chiral superstructure has been shown to be necessary for high enantioselectivity in metalloporphyrin epoxidations, though often at the expense of synthetic flexibility.[28] Recently, a porphyrin−peptide conjugate was also shown to lack the rigidity required to exhibit high enantioselectivity.[29]

Future approaches will be directed toward catalytic studies at low temperatures or toward the synthesis of hosts with more rigidly defined cavities, for example, cavities containing bridging chiral dicarboxylates.

Conclusions

Mixed metalloporphyrin trimers containing both tin(IV) and ruthenium(II) have been synthesized using a stepwise synthetic strategy. The orthogonal coordination behavior of tin(IV) porphyrins and ruthenium(II) porphyrins was exploited to allow

(27) In Ru(TPP)(CO)(py), the ruthenium is pulled 0.079 Å out of the plane of the porphyrin: Little, R. G.; Ibers, J. A. *J. Am. Chem. Soc.* **1973**, *95*, 8583.

(28) (a) Collman, J. P.; Zhang, X.; Lee, V. J.; Uffelman, E. S.; Brauman, J. I. *Science* **1993**, *261*, 1404. (b) Collman, J. P.; Wang, Z.; Straumanis, A.; Quelquejeu, M. *J. Am. Chem. Soc.* **1999**, *121*, 460. (c) Zhang, R.; Yu, W.-Y.; Lai, T.-S.; Che, C.-M. *Chem. Commun.* **1999**, 409.

(29) Geier, G. R.; Sasaki, T. *Tetrahedron* **1999**, *55*, 1859.

stepwise coordination of ligands to selected sites within the host. The tin centers were good attachment points for carboxylates and provided stable hosts having cavities lined with substituents possessing chirality or other desired properties. In this manner, cavities lined with hydrogen-bonding groups or chiral groups were synthesized.

The influence of these carboxylate-lined cavities upon the binding of pyridyl ligands to the ruthenium centers of these hosts was investigated. The rich hydrogen-bonding environment provided by a D-quinate-lined cavity was found to enhance the binding of 4-methanolpyridine to the ruthenium center. However, the chiral carboxylate ligands were not held rigidly enough to enforce any stereocontrol upon the binding of racemic pyridyl ligands.

Similarly, though these hosts were effective catalysts for the epoxidations of alkenes, the presence of chiral carboxylates within the cavities could not induce any enantioselectivity in the epoxidation reactions.

The methodology established in this work allows easy variation of the sizes, shapes, and functionalities of the cavities within these trimers.[30] This accessibility to a wide variety of hosts permits systematic investigations of host/guest or catalyst/substrate interactions.

Experimental Section

NMR spectra were recorded on Bruker AC 250, DPX 250, AM 400, WM 400, and DRX 500 spectrometers, infrared spectra on a Perkin-Elmer 1710 spectrometer, and UV−visible spectra on a Uvikon 810 spectrophotometer. FAB^+/FIB^+ mass spectra were obtained on a Kratos MS-50 spectrometer using a *m*-nitrobenzyl alcohol matrix, and MALDI-TOF mass spectra were recorded on a Kratos Kompact MALDI-2 spectrometer.

Column chromatography was carried out on 60 mesh silica gel or alumina UG1 unless otherwise stated. All solvents were distilled before use. **Ru(CO)Zn$_2$2·Py$_3$T** was prepared according to known procedures,[2] and carbonyl(tetrakis(3,5-di-*tert*-butylphenyl)porphinato)ruthenium(II) was the gift of Dr. N. Bampos. Recrystallization was performed either by layering methanol onto a concentrated solution of the porphyrin in chloroform or by adding hexanes or methanol to a dichloromethane or chloroform solution of the porphyrin, followed by slow removal of the solvent on a rotary evaporator.

The resonances of carbonyls bound to ruthenium porphyrins are too weak to be observed in the ^{13}C NMR spectra and can only be observed if the samples are isotopically enriched with ^{13}CO.[31]

Preparation of Ru(CO)(py)[Sn(OH)$_2$]$_2$2. Ru(CO)Zn$_2$2·Py$_3$T (150 mg, 0.045 mmol) was dissolved in chloroform (225 mL), 20% methanol in TFA (75 mL) was added, and the resulting green solution was stirred for 10 min. The reaction was monitored by UV−visible spectroscopy, and extra TFA was added if needed. The green solution was washed with distilled water (4 × 225 mL); then the red solution was dried with $MgSO_4$. After filtration, the solvent was removed from the red solution under reduced pressure. The residue was dissolved in pyridine (15 mL), and powdered tin(II) chloride dihydrate was added (90 mg, 0.40 mmol). The reaction vessel was protected from light, and the suspension was heated to reflux in air for 2 h. The reaction mixture was allowed to cool, and pyridine was removed under reduced pressure. The red residue was dissolved in chloroform, the solution was filtered through Celite, and the solvent was removed from the filtrate under reduced pressure. The crude **Ru(CO)(py)[SnCl$_2$]$_2$2** was dissolved in chloroform (15 mL), and 10% water on alumina was added (1.5 g). The mixture was stirred for 24 h and filtered, and the solvent was removed from the filtrate. The residue was dissolved in chloroform (15 mL), fresh 10% water on alumina was added (1.5 g), and the resulting mixture was stirred for 24 h. After filtration and removal of the solvent under reduced pressure, the red residue was recrystallized from dichloromethane/hexanes to afford **Ru(CO)(py)[Sn(OH)$_2$]$_2$2** (62 mg, 0.019 mmol, 43% yield). Anal. Calcd for $C_{171}H_{163}N_{13}O_{30}Sn_2Ru\cdot 3H_2O$: C, 63.0; H, 5.1; N, 5.6. Found: C, 63.0; H, 5.1; N, 5.5. IR (dry $CHCl_3$ solution; cm^{-1}): ν_{CO} = 1940 (br); ν_{OH} = 3619 (w). ^{1}H NMR ($CDCl_3$): δ −8.12, −7.83 (2 br s, 3.0H, OH in, OH out); −3.10 (t), −2.82 (q), −2.67 (t), −2.43 (q) (1.2H, bound CH_3CH_2O); 0.84 (d, 2H, α-H of Py); 2.46 (s), 2.58 (s), 2.67 (s) (36H, $-CH_3$); 3.01 (br t, 8H, $-CH_2CH_2CO_2CH_3$ of Ru(Por)); 3.24 (br t, 16H, $-CH_2CH_2CO_2CH_3$ of Sn(Por)); 3.51 (s, 12H, $-CH_2CH_2CO_2CH_3$ of Ru(Por)); 3.72 (s, 24H, $-CH_2CH_2CO_2CH_3$ of Sn(Por)); 4.09 (br t, 10H, $-CH_2CH_2CO_2CH_3$ of Ru(Por) + β-H of Py); 4.40 (br t, 16H, $-CH_2CH_2CO_2CH_3$ of Sn(Por)); 4.78 (t, 1H, γ-H of Py); 7.68−8.65 (m, 24H, aromatic); 9.61 (s, 2H, meso-H of Ru(Por)); 10.65 (s, 4H, meso-H of Sn(Por)). ^{13}C NMR ($CDCl_3$ + Py): δ 15.56, 15.70, 21.70, 21.92, 29.79, 36.40, 36.85, 51.49, 51.82, 74.92, 77.35, 81.67, 89.66, 90.99, 97.78, 98.61, 118.12, 118.46, 118.78, 120.51, 121.76, 122.05, 123.35, 123.76 (Py), 127.94, 128.38, 131.61, 132.41, 132.79, 133.10, 133.34, 133.65, 135.95 (Py), 136.09, 136.17, 137.55, 138.15, 140.06, 140.31, 140.49, 140.69, 141.08, 142.06, 142.28, 142.47, 142.55, 142.86, 143.44, 143.55, 143.90, 149.92 (Py), 173.29, 173.65. λ_{max} ($CHCl_3$)/nm: 405, 417, 525 (sh), 548, 583. MS: no ions detected.

Preparation of Ru(CO)(py)[Sn((*R*)-2-phenylpropionate)$_2$]$_2$2. (*R*)-2-Phenylpropionic acid (3.5 μL, 26 μmol, 4.1 equiv) was added to a solution of **Ru(CO)(py)[Sn(OH)$_2$]$_2$2** (20 mg, 6.4 μmol, 1 equiv) in chloroform (2 mL), and the mixture was briefly heated to reflux. After cooling, the solvent was removed from the solution under reduced pressure, and the red-purple residue that remained was recrystallized from dichloromethane/hexanes and then washed with ether (3 × 0.5 mL) and hexanes to give **Ru(CO)(py)[Sn((*R*)-2-phenylpropionate)$_2$]$_2$2** (11 mg, 3.0 μmol, 48% yield). Anal. Calcd for $C_{207}H_{195}N_{13}O_{34}Sn_2Ru\cdot 2H_2O$: C, 66.0; H, 5.2; N, 4.9. Found: C, 65.8; H, 5.2; N, 4.8. IR (dry $CHCl_3$ solution; cm^{-1}): ν_{CO} = 1940 (s). ^{1}H NMR ($CDCl_3$): δ −1.83 (d, 7.1 Hz, 6H, α-CH_3 of in-Phprop); −1.15 (d, 7.1 Hz, 6H, α-CH_3 of out-Phprop); −0.31 (q, 7.1 Hz, 2H, α-CH of in-Phprop); 0.38 (q, 7.1 Hz, 2H, α-CH of out-Phprop); 0.63 (d, 5.0 Hz, 2H, α-H of Py); 2.34 (s), 2.456 (s), 2.462 (s), 2.57 (s), 2.60 (s) (36H, $-CH_3$); 2.8−3.0 (d of m, 8H, $-CH_2CH_2CO_2CH_3$ of Ru(Por)); 3.07 (br m, 16H, $-CH_2CH_2CO_2CH_3$ of Sn(Por)); 3.40 (s), 3.42 (s) (12H, $-CH_2CH_2CO_2CH_3$ of Ru(Por)); 3.51 (s), 3.52 (s), 3.54 (s), 3.55 (s) (24H, $-CH_2CH_2CO_2CH_3$ of Sn(Por)); 3.99 (m, 14H, $-CH_2CH_2CO_2CH_3$ of Ru(Por) + *o*-CH of in-Phprop + β-H of Py); 4.31 (m, 17H, $-CH_2CH_2CO_2CH_3$ of Sn(Por) + γ-H of Py); 4.63 (d, 7.3 Hz, 4H, *o*-CH of out-Phprop); 5.88 (t, 7.4 Hz, 4H, *m*-CH of in-Phprop); 6.28 (t, 2H, *p*-CH of in-Phprop); 6.44 (t, 7.6 Hz, 4H, *m*-CH of out-Phprop); 6.71 (t, 7.3 Hz, 2H, *p*-CH of out-Phprop); 7.60−8.30 (m, 24H, aromatic); 9.47 (s, 2H, meso-H of Ru(Por)); 10.43 (s), 10.45 (s) (4H, meso-H of Sn(Por)). λ_{max} ($CHCl_3$)/nm: 414, 545, 581. MS: no ions detected.

Preparation of Ru(CO)(py)[Sn((*R*)-mandelate)$_2$]$_2$2. (*R*)-Mandelic acid (5.80 mg, 38.1 μmol, 4.0 equiv) was added to a solution of **Ru(CO)(py)[Sn(OH)$_2$]$_2$2** (30.0 mg, 9.42 μmol, 1.0 equiv) in chloroform (3 mL), and the mixture was briefly heated to reflux. After cooling, the solvent was removed from the solution under reduced pressure. The red-purple residue that remained was recrystallized from dichloromethane/hexanes and washed with hexanes to afford **Ru(CO)(py)[Sn((*R*)-mandelate)$_2$]$_2$2** (29 mg, 7.8 μmol, 80% yield). Anal. Calcd for $C_{203}H_{187}N_{13}O_{38}Sn_2Ru\cdot CH_2Cl_2\cdot 2H_2O$: C, 63.5; H, 4.8; N, 4.7. Found: C, 63.4; H, 5.0; N, 4.8. IR (dry $CHCl_3$ solution; cm^{-1}): ν_{CO} = 1940 (br, s); ν_{OH} = 3450 (br). ^{1}H NMR ($CDCl_3$): δ 0.61 (d, 5.2 Hz, 2H, α-H of Py); 0.98 (s, 2H, α-CH of in-Mand); 1.67 (s, 2H, α-CH of out-Mand); 2.35 (s), 2.36 (s), 2.49 (s), 2.50 (s), 2.61 (s), 2.62 (s), (36H, $-CH_3$); 2.8−3.0 (d of m, 8H, $-CH_2CH_2CO_2CH_3$ of Ru(Por)); 3.08 (br m, 16H, $-CH_2CH_2CO_2CH_3$ of Sn(Por)); 3.406 (s), 3.412 (s) (12H, $-CH_2CH_2CO_2CH_3$ of Ru(Por)); 3.54 (s), 3.56 (s), 3.57 (s), 3.58 (s) (24H, $-CH_2CH_2CO_2CH_3$ of Sn(Por)); 3.94 (m, 10H, $-CH_2CH_2CO_2CH_3$ of Ru(Por) + β-H of Py)); 4.16 (d, 7.6 Hz, 4H, *o*-CH of in-Mand); 4.36 (m, 16H, $-CH_2CH_2CO_2CH_3$ of Sn(Por)); 4.54 (t, 5.2 Hz, 1H, γ-H of Py); 4.79 (d, 7.6 Hz, 4H, *o*-CH of out-Mand); 5.97 (t, 7.6 Hz, 4H, *m*-CH of in-Mand); 6.39 (t, 2H, *p*-CH of in-Mand); 6.51 (t, 4H, 7.6

(30) The complementary coordination properties of Sn(IV), Ru(II), and Zn(II) were recently used in this laboratory to create mixed-metal porphyrin trimers of a very different geometry under thermodynamic control: Kim, H.-J.; Bampos, N.; Sanders, J. K. M. *J. Am. Chem. Soc.* **1999**, *121*, 8120.

(31) Eaton, S. S.; Eaton, G. R. *Inorg. Chem.* **1976**, *15*, 134.

Hz, *m*-CH of out-Mand); 6.82 (t, 2H, *p*-CH of out-Mand); 7.05 (br s, OH); 7.70−8.30 (m, 24H, aromatic); 9.46 (s, 2H, meso-H of Ru(Por)); 10.45 (s), 10.53 (s) (4H, meso-H of Sn(Por)). ^{13}C NMR ($CDCl_3$): δ 15.52, 15.62, 21.71, 36.20, 36.63, 51.40, 51.74, 69.10, 69.78, 74.79, 77.20, 81.42, 89.36, 91.12, 97.55, 97.61, 98.35, 118.10, 118.21, 119.08, 120.42, 121.52, 121.67, 123.13, 123.35, 123.75, 125.32, 125.66, 125.91, 126.36, 127.84, 128.21, 131.39, 132.29, 132.71, 133.33, 133.52, 135.99, 136.22, 137.02, 137.82, 137.89, 138.39, 139.92, 140.19, 140.30, 140.37, 140.42, 140.86, 141.20, 141.38, 142.48, 142.77, 143.00, 143.28, 143.82, 143.87, 144.01, 144.05, 167.74, 168.13, 173.16, 173.62. λ_{max} ($CHCl_3$)/nm: 415, 545, 581. MS: no ions detected.

Preparation of Ru(CO)(py)[Sn((*S*)-(+)-6-methoxy-α-methyl-2-naphthaleneacetate)$_2$]$_2$2. (*S*)-(+)-6-Methoxy-α-methyl-2-naphthaleneacetic acid (Naproxen) (1.54 mg, 6.69 μmol, 4.3 equiv) was added to a solution of **Ru(CO)(py)[Sn(OH)$_2$]$_2$2** (4.92 mg, 1.55 μmol) in chloroform (2 mL), and the mixture was briefly heated to reflux. After cooling, the solvent was removed from the solution under reduced pressure to give **Ru(CO)(py)[Sn((*S*)-(+)-6-methoxy-α-methyl-2-naphthaleneacetate)$_2$]$_2$2** (6 mg, 1.5 μmol, 96% yield). ^{1}H NMR ($CDCl_3$): δ −1.73 (d, 6.9 Hz, 6H, α-CH_3 of in-Naphth); −1.03 (d, 6.9 Hz, 6H, α-CH_3 of out-Naphth); −0.28 (q, 7.3 Hz, 2H, α-CH of in-Naphth); 0.47 (q, 7.1 Hz, 2H, α-CH of out-Naphth); 0.58 (d, 5.0 Hz, 2H, α-H of Py); 2.30 (s), 2.35 (s), 2.45 (s) (36H, $-CH_3$); 2.97 (m, 24H, $-CH_2CH_2CO_2CH_3$ of Ru(Por) and Sn(Por)); 3.40 (s), 3.41 (s) (12H, $-CH_2CH_2CO_2CH_3$ of Ru(Por)); 3.50 (s), 3.520 (s), 3.524 (s), 3.58 (s) (24H, $-CH_2CH_2CO_2CH_3$ of Sn(Por)); 3.93, 4.21 (br m, ∼30H, $-CH_2CH_2CO_2CH_3$ of Ru(Por) subunit + $-CH_2CH_2CO_2CH_3$ of Sn(Por) subunits + Ar H and $ArOCH_3$ of Naphth + β,γ-H of Py)); 4.43 (d), 4.62 (s), 6.38 (d), 6.5−7.1 (m) (20H, Ar H and $ArOCH_3$ of Naphth); 7.58−8.25 (m, 24H, aromatic); 9.47 (s, 2H, meso-H of Ru(Por)); 10.27 (s), 10.32 (s) (4H, meso-H of Sn(Por)). MS: no ions detected.

Preparation of Ru(CO)(py)[Sn(D-quinate)$_2$]$_2$2. D-(−)-Quinic acid (1.24 mg, 6.45 μmol, 4.1 equiv) was added to a solution of **Ru(CO)(py)[Sn(OH)$_2$]$_2$2** (5.00 mg, 1.57 μmol, 1 equiv) in chloroform/methanol (2:1, 1 mL), and the mixture was briefly heated to reflux. After cooling, the solvent was removed from the solution under reduced pressure, and the red-purple residue that remained was redissolved in chloroform. Filtration through cotton wool removed excess quinic acid. The solvent was removed from the filtrate under reduced pressure to give **Ru(CO)(py)[Sn(D-quinate)$_2$]$_2$2** as a red-purple solid (5 mg, 1.3 μmol, 82% yield). ^{1}H NMR ($CDCl_3$): δ −2.43 (t, 12.0 Hz, 2H, 6-H of axial in-Quin); −2.28 (d, 14.1 Hz, 2H, 2-H of axial in-Quin); −1.81 (t, 12.2 Hz, 2H, 6-H of axial out-Quin); −1.63 (d, 11.6 Hz, 2H, 2-H of axial out-Quin); −1.45 (d, 15.6 Hz, 2H, 2-H of equatorial in-Quin); −1.41 (d, 9.7 Hz, 2H, 6-H of equatorial in-Quin); −0.88 (d, 12.4 Hz, 2H, 6-H of equatorial out-Quin); −0.80 (d, 14.5 Hz, 2H, 2-H of equatorial out-Quin); 0.61 (d, 5.0 Hz, 2H, α-H of Py); 0.88 (t, 6.8 Hz, 2H, 3-H of equatorial in-Quin); 1.20−2.00 (∼10H, br s + m, −OH + 4-H of axial Quin + 5-H of equatorial in-Quin); 2.33 (s), 2.34 (s), 2.53 (s), 2.64 (s) (38H, $-CH_3$ + 5-H of axial out-Quin); 2.8−3.0 (d of m, 8H, $-CH_2CH_2CO_2CH_3$ of Ru(Por)); 3.11 (q, 16H, $-CH_2CH_2CO_2CH_3$ of Sn(Por)); 3.43 (s), 3.44 (s) (12H, $-CH_2CH_2CO_2CH_3$ of Ru(Por)); 3.53 (s), 3.55 (s) (24H, $-CH_2CH_2CO_2CH_3$ of Sn(Por)); 3.97 (m, 8H, $-CH_2CH_2CO_2CH_3$ of Ru(Por)); 4.13 (d, 7.0 Hz, 2H, β-H of Py); 4.39 (m, 16H, $-CH_2CH_2CO_2CH_3$ of Sn(Por)); 4.97 (t, 7.7 Hz, 1H, γ-H of Py); 7.68−8.23 (m, 24H, aromatic); 9.49 (s, 2H, meso-H of Ru(Por)); 10.72 (s, 4H, meso-H of Sn(Por) subunits). MS: no ions detected.

Preparation of (±)-1-Phenyl-1-pyridylpropan-1-ol.[32] Clean dry magnesium turnings (0.27 g, 11 mmol) and a crystal of iodine were added to a 100 mL three-necked round-bottomed flask equipped with a reflux condenser and a pressure-equilibrating dropping funnel, and the system was placed under argon. The magnesium turnings were gently heated under vacuum before 4-benzoylpyridine (1.83 g, 10 mmol) was added to the dropping funnel against a flow of argon. Dry THF (7 mL) containing ethyl iodide (1.56 g, 10 mmol) was added to the magnesium turnings, initially giving a yellow color, which rapidly disappeared with the evolution of heat. The colorless solution was stirred at 15 °C for 30 min and then at 50 °C for 1 h, resulting in the dissolution of most of the magnesium turnings. The ketone was dissolved in dry THF (17 mL) to give a pale yellow solution. The Grignard solution was cooled to 15 °C with a water bath, and more dry THF was added (15 mL). The ketone solution was added dropwise over the period of 1 h, which produced a brown solution and a green-white solid. After all of the ketone solution had been added, the mixture was stirred at 15 °C for 1 h and then heated to reflux overnight. The resulting mixture was allowed to cool, and saturated NH_4Cl solution was added (7 mL), followed by distilled water (33 mL). The product was extracted from the aqueous phase with ethyl acetate (100 mL, 2 × 33 mL), the extract was dried ($MgSO_4$) and filtered, and the solvent was removed under reduced pressure to give a yellow oil. TLC indicated a mixture (silica/diethyl ether), but crystallization of the oil from hot acetonitrile gave white crystals. The solid was filtered off and washed three times with cold acetonitrile and once with hexanes to give (±)-1-phenyl-1-pyridylpropan-1-ol as a white crystalline solid (362 mg, 1.70 mmol, 17% yield). Anal. Calcd for $C_{14}H_{15}NO$: C, 78.8; H, 7.1; N, 6.6. Found: C, 78.6; H, 7.1; N, 6.7. IR (Nujol mull; cm^{-1}): ν_{OH} = 3143 (s), 1604 (s), 1278, 1224, 1200, 1134, 1071, 1062, 1006, 991, 827, 764, 722, 699 (s). ^{1}H NMR ($CDCl_3$): δ 0.90 (t, 7.3 Hz, 3H, $-CH_3$); 2.32 (m, 3H, $-CH_2-$ + OH); 7.26−7.44 (m, 7H, β-H of Py + H of Ph); 8.51 (d, 5.8 Hz, 2H, α-H of Py). ^{13}C NMR ($CDCl_3$): δ 7.92 (CH_3), 33.93 (CH_2), 77.61 (C*), 121.18 (CH), 126.04 (CH), 127.37 (CH), 128.44 (CH), 145.76 (C*), 149.40 (CH), 155.97 (C*). λ_{max} ($CHCl_3$)/nm): 227. Mass spectral data (*m*/*z*): calculated for $C_{14}H_{15}NO$ 213; FIB^+ found 214.3 ($[M + H]^+$).

Preparation of Methyl 4-Vinylbenzoate.[33] Concentrated sulfuric acid (3 drops) was added to a solution of 4-vinylbenzoic acid (100 mg, 0.67 mmol) in methanol (10 mL), and the mixture was heated to reflux for 4 h. The solution, diluted with chloroform (10 mL), was then washed with saturated sodium bicarbonate solution (10 mL). The aqueous layer was extracted with chloroform (10 mL), and the combined organic phases were washed with distilled water (20 mL) and dried ($MgSO_4$). The solution was filtered, and the solvent was removed under reduced pressure to afford a yellow oil, which was then purified by column chromatography (dichloromethane/silica). The solvent was removed from the fast running product band under reduced pressure to give methyl 4-vinylbenzoate as a white crystalline solid (90 mg, 0.60 mmol, 82% yield). Anal. Calcd for $C_{10}H_{10}O_2$: C, 74.1; H, 6.2. Found: C, 73.2; H, 6.1. ^{1}H NMR ($CDCl_3$): δ 3.92 (s, 3H, $-OCH_3$); 5.38 (d, 11.0 Hz, 1H, $=CH_2$); 5.86 (d, 17.1 Hz, 1H, $=CH_2$); 6.76 (d of d, 10.9 Hz, 17.6 Hz, 2H, $=CH-Ar$); 7.46 (d, 8.4 Hz, 2H, Ar H); 8.00 (d, 8.4 Hz, 2H, Ar H). ^{13}C NMR ($CDCl_3$): δ 52.04 (CH_3), 116.45 ($=CH_2$), 126.10 (CH), 129.29 (CH), 129.88 (C*), 136.03 (CH), 141.93 (C*), 166.86 (C=O). Mass spectral data (*m*/*z*): calculated for $C_{10}H_{10}O_2$ = 162; FIB^+ found 163 ($[M + H]^+$).

Preparation of *N*-(4-Nitrobenzyl)-4-vinylbenzamide. Dry triethylamine (1 mL) was added to a solution of 4-vinylbenzoic acid (100 mg, 0.68 mmol, 1 equiv) under argon in freshly distilled dry dichloromethane (10 mL), followed by freshly distilled thionyl chloride (100 μL, 1.35 mmol, 2 equiv). The initially yellow mixture became black after 5 min. The black mixture was stirred at room temperature for 2 h, 4-nitrobenzylamine hydrochloride (127 mg, 0.67 mmol, 1 equiv) and DMAP (16.5 mg, 0.14 mmol, 0.2 equiv) were then added, and the solution was stirred for 1 h. The resulting mixture was washed with distilled water (2 × 10 mL), the organic layer was dried ($MgSO_4$) and filtered, and the solvent was removed from the filtrate under reduced pressure. The residue was purified by column chromatography (silica/diethyl ether), the main product fraction was collected, and the solvent was removed under reduced pressure. The yellow residue was recrystallized twice from hot toluene to give *N*-(4-nitrobenzyl)-4-vinylbenzamide as yellow needles (94 mg, 0.33 mmol, 49% yield). Anal. Calcd for $C_{16}H_{14}N_2O_3$: C, 68.1; H, 5.0; N, 6.9. Found: C, 68.0; H, 5.1; N, 6.7. IR (Nujol mull; cm^{-1}): ν_{NH} = 3237 (s); ν_{CO} = 1637 (s), 1605, 1545, 1515 (s), 1352 (s), 1316 (s), 1300, 1251, 1114, 1051, 988, 918, 859, 799, 772, 736, 721. ^{1}H NMR ($CDCl_3$): δ 4.76 (d, 6.1 Hz, 2H, $-CH_2-$); 5.39 (d, 11.0 Hz, 1H, $=CH_2$); 5.86 (d, 17.9 Hz, 1H, $=CH_2$); 6.61 (br s, 1H, NH); 6.76 (d of d, 10.9 Hz, 17.6 Hz, 1H, $=CH-R$); 7.50 (d of d, both 8.3 Hz, 4H, Ar CH); 7.78 (d, 8.4 Hz, 2H, Ar CH); 8.20 (d, 8.7 Hz, 2H, Ar CH). ^{13}C NMR ($CDCl_3$): δ 43.09 (CH_2), 116.21 ($=CH_2$),

(32) Davies, A. G.; Kenyon, J.; Thaker, K. *J. Chem. Soc.* **1956**, 3395.

(33) Marvel, C. S.; Overberger, C. G. *J. Am. Chem. Soc.* **1945**, *67*, 2250.

123.8 (CH), 126.34 (CH), 127.42 (CH), 128.21 (CH), 132.68 (C*), 135.79 (CH), 141.05 (C*), 146.19 (C*), 147.15 (C*), 167.74 (C═O). λ_{max} ($CHCl_3$)/nm: 269. Mass spectral data (*m*/*z*): calculated for $C_{16}H_{14}N_2O_3$ 282: FIB^+ found 283.1 ($[M + H]^+$).

Binding of 4-Methanolpyridine to Carbonyl(methanol)(tetrakis-(3,5-di-*tert*-butylphenyl)porphinato)ruthenium(II). Pyridine (3.04 mg, 38.4 μmol) was added of a solution of carbonyl(methanol)(tetrakis-(3,5-di-*tert*-butylphenyl)porphinato)ruthenium(II) (5.0 mg, 4.1 μmol) in $CDCl_3$ (500 μL). Aliquots of a solution of 4-methanolpyridine (8.47 mg, 77.6 μmol) in $CDCl_3$ (200 μL) were added to the porphyrin solution, and a 250 MHz ^{1}H NMR spectrum was recorded after each addition. The Ru(Por)·Py:Ru(Por)·$PyCH_2OH$ ratio was most easily determined by comparing the integration of the γ-proton (pyridine) resonance to the integration of the β-proton (pyridine + 4-methanolpyridine) resonances.

Binding of 4-Methanolpyridine to Ru(CO)(py)[Sn(D-quinate)$_2$]$_2$2. Pyridine (3.05 mg, 38.6 μmol) was added of a solution of **Ru(CO)(py)[Sn(D-quinate)$_2$]$_2$2** (6.2 mg, 1.6 μmol) in $CDCl_3$ (610 μL). Aliquots of a solution of 4-methanolpyridine (9.02 mg, 82.7 μmol) in $CDCl_3$ (200 μL) were added to the porphyrin solution, and a 500 MHz ^{1}H NMR spectrum was recorded after each addition. The trimer·Py:trimer·$PyCH_2OH$ ratio could easily be determined from integration of the respective ruthenium meso-H signals.

Binding of Racemic Pyridines to Chiral Trimers. For the soluble (±)-1-phenyl-1-pyridylpropan-1-ol, a 100-fold excess of the ligand was added to each solution of chiral trimer in $CDCl_3$. For the less soluble (±)-4-(4-pyridyl)-*trans*-cyclohexane-1,2-diol, the ligand was added to each $CDCl_3$ solution of chiral trimer until the solution was saturated.

Oxidation of Styrene and Styrene Derivatives with Chiral Ru(CO)(py)[Sn(carboxylate)$_2$]$_2$2 Trimers. The catalyst (**Ru(CO)3**, 1.2 mg, 1.0 μmol, or **Ru(CO)(py)[Sn(carboxylate)$_2$]$_2$2**, 3.7 mg, 1.0 μmol) was added to a solution of 2,6-dichloropyridine *N*-oxide (29.5 mg, 180 μmol) in benzene-d_6 (2 mL). The mixture was stirred while being protected from light; then *m*-chloroperoxybenzoic acid (86%, 0.7 mg, 3.5 μmol) was added. The resulting red solution was stirred while being protected from light for 20 min before the substrate was added (180 μmol: styrene, 17.7 mg; methyl 4-vinylbenzoate, 27.6 mg; *N*-(4-nitrobenzyl)-4-vinylbenzamide, 48.0 mg). The reaction mixture was protected from light while being stirred. Reaction progress was monitored by ^{1}H NMR spectroscopy. Enantiomeric excesses were determined by adding (+)-Eu(hfc)$_3$ to the NMR sample until the resonances of the diastereomeric complexes could be clearly resolved.[34]

Acknowledgment. We thank Mr. P. Loveday and Mr. S. Wilkinson (UCL, Cambridge) for $Ru_3(CO)_{12}$, Mr. C. Sporikou (UCL, Cambridge) for benzyl 4-(2-(methoxycarbonyl)ethyl)-3,5-dimethylpyrrole-2-carboxylate, Dr. E. Levy for (±)-4-(4-pyridyl)-*trans*-cyclohexane-1,2-diol, Dr. N. Bampos for NMR spectra and supplies of carbonyl(tetrakis(3,5-di-*tert*-butylphenyl)porphinato)ruthenium(II), Dr. L. Twyman for MALDI-TOF spectra, the EPSRC Mass Spectrometry Service for FAB mass spectra, and Dr. J. Hawley for useful advice. Phoenix Pharm Distributors, the Ethyl Corp., the Cambridge Commonwealth Trust, and the NZVCC provided generous financial support.

IC0004129

(34) Groves, J. T.; Myers, R. S. *J. Am. Chem. Soc.* **1983**, *105*, 5791.